EPSC Abstracts
Vol. 10, EPSC2015-51, 2015
European Planetary Science Congress 2015

Methanol photochemistry as a source of complex organic molecules in cometary environments

N. Abou Mrad, F. Duvernay, T. Chiavassa and G. Danger
Aix-Marseille University, CNRS, PIIM, UMR 7345, 13013 Marseille, FRANCE
(gregoire.danger@univ-amu.fr)

Abstract

This contribution focuses on the identification and quantification of Volatile Organic Compounds (VOC) subliming after the warm-up of photo-processed methanol ice analogs using the VAHIIA experimental set-up. Data obtained will help elucidating the presence of molecules in astrophysical environments such as comets, as well as estimating the detectability of methanol photoproducts in these environments based on a quantitative approach.

1. Introduction

Comets are of prime interest in the study of the origin of the planetary organic matter since they have preserved for a part the original material of the solar nebula which subsequently led to our solar system. The determination of organics in comets is an important objective for understanding the chemical evolution occurring during the solar system formation. However, probing such objects is a difficult task and data interpretation is quite complex. The chemical evolution of organic matter occurs also mostly in low- and high-mass protostellar envelopes known as hot cores and hot corinos. These regions are extensively observed using radio astronomy to identify their content in complex organic molecules, but here also data interpretation is often ambiguous. For enhancing data interpretations obtained from cometary missions and understanding the chemical reactivity that occurs in cometary environments and in hot cores, laboratory experiments have been developed. They consist in recreating the astrophysical environment where astrophysical ices are processed. Briefly, ice analogs are formed at low temperature (10-80 K) and pressure (10^{-8} mbar) with the most abundant molecules detected in interstellar and cometary ices. They are then submitted to energetic processes such as ultraviolet photons simulating the internal ultraviolet field inside cold molecular clouds. Afterwards the ice analog is warmed-up leading to the desorption of volatile compounds enriching the gas phase of the vacuum chamber. The analysis of compounds released in the gas phase can help explaining the presence and formation of such molecules in astrophysical environments, and orient the search for these compounds by the scientific community.

Among the most abundant molecules detected in astrophysical ices, MeOH is important, since it is the most abundant source of reduced carbon available within these icy grains. Therefore, understanding the chemistry related to this molecule is an important challenge that would give essential clues on the cometary chemistry and on molecules that could be detected in this environment. Infrared spectroscopy coupled to Temperature Program Desorption [1] as well as experiments using single photoionization reflectron time of flight mass spectrometry [2] were used to identify 15 volatile organic compounds from methanol photo-processed ices while more molecules are expected. In this contribution, we have used the VAHIIA system based on a gas chromatography coupled to mass spectrometry approach to screen and quantify photoproducts formed after the VUV irradiation and the subsequent warming of a pure CH_3OH ice.

2. VAHIIA experimental set-up

When the ice analog formed in the high vacuum chamber is warmed-up, sublimating species are pumped to a **preconcentration unit** directly connected to the chamber [3]. This developed unit has two main objectives: firstly, preconcentrating analytes prior to the GC analysis; secondly, reaching a pressure sufficient to provide a GC analysis. Concretely, species are pumped out of the chamber using pneumatic valves and are then stacked in a

preconcentration loop submerged in liquid nitrogen. After preconcentration, the loop is then rapidly warmed-up to 70°C. Helium is then introduced in the loop to increase sample pressure and facilitate analyte transfer to the **injection unit**. This latter was developed in collaboration with Interscience Belgium and allows the introduction of the gaseous sample coming from the preconcentration unit into the GC injector classically conceived for liquid sample injections (Figure 1).

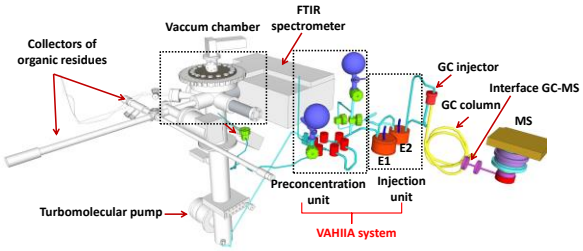

Figure 1: The VAHIIA system for VOC analysis.

3. Results

The GC-MS chromatogram of the photo-processed CH_3OH ice shows plethoras of peaks, which we identified based on their retention time and mass spectrum fragmentation pattern [4]. Identified photoproducts are constituted of 2 to 6 carbon atoms with various chemical functions, such as aldehydes (C2-C6), alcohols (C2-C5), ketones (C3-C6), esters (C2-C6), ethers (C3-C5) or carboxylic acids (C2). Almost all C3 to C6 compounds were not identified previously, highlighting the power of the VAHIIA experimental set-up to translate the complexity of photoprocessed ices. In addition to the identification process, we have focused on the quantification of all C1, C2 and C3 compounds that have been assigned since they are the most abundant, along with few C4 photoproducts. Our objective is to provide data on CH_3OH photo-dissociation, mainly the abundance of photoproducts with respect to the irradiated fraction of CH_3OH (branching ratios) and to the remaining CH_3OH fraction after irradiation (observational ratio).These results give essential information for helping data interpretation of the current Rosetta mission, as well as for assessing the different photo-dissociation pathways and diagnosing the conditions of molecule formation.

Acknowledgements

The "Centre National d'Études Spatiales" (C.N.E.S) and the "Agence Nationale de la Recherche" through the ANR-VAHIIA (ANR-12-JS08-0001-01) are acknowledged for financial support. We also thank Interscience Belgium for technical support.

References

[1] Oberg, K. I., Garrod, R. T., van Dishoeck, E. F., & Linnartz, H., *A&A. 2009, 504, 891-913*

[2] Maity, S., Kaiser, R. I., & Jones, B. M., *Phys. Chem. Chem. Phys. 2015, 17, 3081-3114*

[3] Abou Mrad, N., Duvernay, F., Chiavassa, T. & Danger, G., *Anal. Chem. 2014, 86, 8391-8399*

[4] Abou Mrad, N., Duvernay, F., Chiavassa, T. & Danger, G., *under submission*

EPSC Abstracts
Vol. 10, EPSC2015-88, 2015
European Planetary Science Congress 2015

UV cometary observations by SPICAV on Venus Express

J-Y.Chaufray and J-L. Bertaux
LATMOS-IPSL, CNRS, Guyancourt, France

Abstract

Several campaigns of cometary observations have been performed by the UV spectrometer SPICAV from 2012 to 2014. In this presentation we will present the results obtained for the 6 observed comets and their water sublimation rates as a function of the sun distance.

1. Introduction

The production rates of water of several comets has been derived from observations of the cometary H Lyman-α emission (e.g. 1, 3). SPICAV-UV is the UV spectrometer of the Venus Express mission dedicated to the study of the venusian atmosphere (2). The orbit of Venus Express is highly elliptic with an apocenter at 66000 km above the planet center. At apocenter, the venusian emissions are very weak and observations of other objects of the solar system are possible.

2. SPICAV Observations

The observed comets are indicated in Table 1.

Comet	Time period of observations	Number of runs
96P MachHolz 1	06/07/2012 – 23/07/2012	15
C/2011 L4 PanStarrs	30/01/2013 – 15/03/2013	38
C/2012 S1 ISON	22/10/2013 – 05/01/2014	99
C/2014 E2 Jacques	21/07/2014 – 15/08/2014	33
C/2012 K1 PanStarrs	24/08/2014 – 07/09/2014	26
C/2013 V5 Oukaimeden	10/10/2014 – 12/10/2014	15

Table 1 : List of the comets observed by SPICAV-UV/VEX

The cometary Lyman-α emission of atomic hydrogen has been observed for all the comets, for some comets (e.g. ISON), OH lines have also been observed near 308 nm. An example of cometary specrum of ISON measured by SPICAV-UV is displayed on Fig. 1

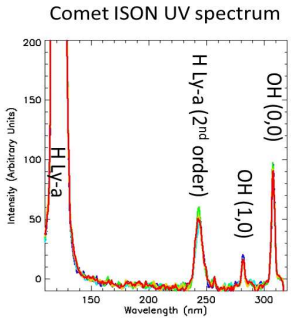

Fig. 1 Example of UV spectrum of the comet ISON measured by SPICAV-UV

Several modes of observations were used to map the emissions of the comets, large zigzag motions of the pointing were performed to derive an extended map with a low spatial resolution and small shift of the pointing were used to obtain less extended maps but with a better spatial resolution. Example of a Lyman-α map of ISON with a good spatial resolution is presented on Fig. 2

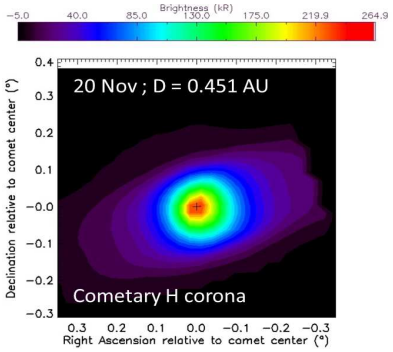

Fig. 2 Example of map of the Lyman-α emission around ISON obtained by SPICAV-UV

From these emissions, using the vectorial model of Festou (4), we have estimated the water production rates of the comets at different distances to the sun.

3. Summary and Conclusions

6 comets have been observed successfully by SPICAV-UV from 2012 to 2014. For all comets, the hydrogen Lyman-α emission is detected and for some of them (e.g. ISON), the OH emission is also detected. Spatial maps with an unp of these two emissions have been derived and will be presented as well as a first estimate of the water sublimation as a function of the sun distance.

Acknowledgements

Venus Express was a space mission from European Space Agency (ESA). We wish to express our gratitude to all ESA members who participated in this successful mission and in particular H. Svedhem, D. McCoy, O. Witasse, A. Accomazzo, and J. Louet. We thank CNRS and CNES for funding SPICAV in France.

References

[1] Bertaux, J-L. et al., *A&A*, **25**, 415-430, 1973

[2] Bertaux, J-L. et al., *Planet. Space Sci.*, **55**, 1673-1700, 2007

[3] Combi, M.R. et al., *Icarus*, **144**, 191-202, 2000

[4] Festou, M.C., *A&A*, **95**, 69-79, 1981

EPSC Abstracts
Vol. 10, EPSC2015-126, 2015
European Planetary Science Congress 2015

The giant comet 29P/Schwassmann–Wachmann 1 as seen in the thermal infrared by the AKARI space telescope

D. Perna (1), C. Feller (1,2), E. Mazzotta Epifani (3,4), S. Fornasier (1,2), D. Bockelée-Morvan (1), Ootsubo T. (5), Kawakita H. (6), Usui F. (5) and Ishiguro M. (7)
(1) LESIA – Observatoire de Paris, France, (2) Université Paris Diderot – Paris 7, France, (3) INAF – Osservatorio Astronomico di Capodimonte, Italy, (4) INAF – Osservatorio Astronomico di Roma, Italy, (5) University of Tokyo, Japan, (6) Kyoto Sangyo University, Japan, (7) Seoul National University, Korea (davide.perna@obspm.fr / Fax: +33 145077144)

Abstract

We present thermal infrared images (15 and 24 μm) and spectra (1.8-12.9 μm) of the giant comet 29P/Schwassmann–Wachmann 1 (29P hereafter), acquired in 2007 with the Japanese AKARI space telescope. Despite orbiting at around 6 AU from the Sun, the comet showed a sustained activity. We investigated its nucleus properties (size, albedo, rotation), as well as its dust and gas production.

1. Introduction

Comet 29P is one of the largest ever discovered and is known to present a recursive activity, with about 6-7 episodes per year [10]. Orbiting the Sun on a low eccentric orbit with an aphelion of 6.25 AU and a perihelion of 5.72 AU, this object gives us the possibility to analyse in a comprehensive way a "far" cometary environment, at heliocentric distances where water sublimation cannot trigger the activity and the sublimation of other surface volatiles, such as CO, is responsible for the presence of a coma. Indeed, carbon monoxide has been detected by several authors in the coma of 29P and is thought to be its primary driver gas (e.g., [3]).

We used the InfraRed Camera (IRC) [7] onboard the AKARI telescope to characterize the physical properties of 29P, as discussed in the following sections.

2. Data reduction

Imaging frames at 15 and 24 μm have been pre-reduced using the calibration files presented in [1]. Further reduction steps included: removal of cosmic rays and instrumental artifacts; image deconvolution (Fig. 1) using the "maximum likelihood" algorithm based on the Lucy-Richardson method [5],[8]; shifting and adding the frames to produce the final 15 and 24 μm images, that have been flux-calibrated taking into account both aperture and color corrections.

Fig. 1: 15-μm image (2.51″/pixel) of 29P, before (left) and after (right) a "maximum likelihood" deconvolution.

3. Results

After both radial normalization and Angular Differential Imaging (Fig. 2) techniques, the images of 29P show the presence of three dust jets extending up to about 2×10^5 km from the nucleus. Assuming that the curvature of the jets is due to the rotation of the nucleus, and using a dust ejection velocity of 20 m/s, the rotational period is found to be 23±14 h.

Comparing the radial profile of 29P with that of star HD37122, we could discriminate between the nucleus and coma contributions to the detected flux in comet images at 15 and 24 μm. After having combined our measurements with those obtained for 29P at 8 μm by [9], we applied the Standard Thermal Model [4] to derive an estimation of the size and the

albedo of the nucleus, finding values of 56.3±3.8 km and 2.3±0.3%, respectively.

Based on [2], we modelled the thermal emission of the coma assuming it is composed of amorphous carbon grains in the 0.1-100 μm size range. Assuming that the grains are ejected with an average velocity of 20 m/s, we derived a dust production rate of about 660 kg/s, in agreement with previous results by [6], who had found a dust loss mass rate in the range of 300-900 kg/s.

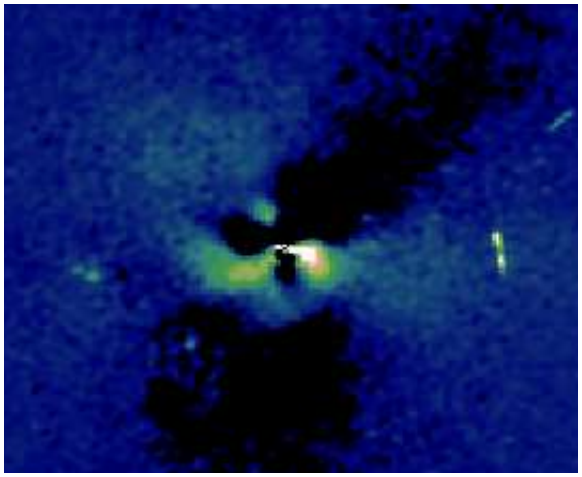

Fig. 2: Angular Differential Imaging applied (45° rotation) to the 24-μm image of 29P. The image resolution is ~10.5×10^3 km/pixel.

4. Summary and work in progress

At the time of writing we are:

- Refining the analysis of the imaging data. In particular we will consider different grain compositions (e.g., olivine and pyroxene) to improve the estimation of the dust production rate.

- Analysing the spectral data. These seem to suggest the presence of both water and carbon monoxide, and possibly also of carbon dioxide.

Our preliminary results will be presented and discussed.

References

[1] Arimatsu, K., Onaka,T., Sakon, I., et al. : Characterization and Improvement of the Image quality of the Data Taken with the Infrared Camera (IRC) Mid-Infrared Channels on Board AKARI, PASJ, 123, pp. 981-995, 2011.

[2] Gicquel, A., Bockelée-Morvan, D., Zakharov, V. V., et al.: Investigation of dust and water ice in comet 9P/Tempel 1 from Spitzer observations of the Deep Impact event, A&A, 542, A119, 16 pp., 2012.

[3] Gunnarsson, M., Bockelée-Morvan, D., Biver, N., Crovisier, J., & Rickman, H.: Mapping the carbon monoxide coma of comet 29P/Schwassmann-Wachmann 1, A&A, 484, pp. 537-546, 2008.

[4] Lebofsky, L. A., & Spencer, J. R.: Radiometry and a thermal modeling of asteroids. In: Asteroids II, Univ. of Arizona Press, pp. 128-147, 1989.

[5] Lucy, L. B.: An iterative technique for the rectification of observed distributions, Astronomical Journal, 79, pp. 745-754, 1974.

[6] Moreno F: The Dust Environment of Comet 29P/Schwassmann-Wachmann 1 From Dust Tail Modeling of 2004 Near-Perihelion Observations, ApJ Supplement, 183, pp. 33-45, 2009.

[7] Onaka, T., Matsuhara, H., Wada, T., et al.: The Infrared Camera (IRC) for AKARI -- Design and imaging performance, PASJ, 59, S401-S410, 2007.

[8] Richardson, W. H.: Bayesian-Based Iterative Method of Image Restoration, Journal of the Optical Society of America, 62, pp. 55-59, 1972.

[9] Stansberry, J. A., Van Cleve, J., Reach, W. T., et al.: Spitzer Observations of the Dust Coma and Nucleus of 29P/Schwassmann-Wachmann 1, ApJ Supplement Series, 154, pp. 463-468, 2004.

[10] Trigo-Rodríguez, J. M., García-Melendo, E., Davidsson, B. J. R., et al.: Outburst activity in comets. I. Continuous monitoring of comet 29P/Schwassmann-Wachmann 1, A&A, 485, pp. 599-606, 2008.

EPSC Abstracts
Vol. 10, EPSC2015-315, 2015
European Planetary Science Congress 2015

Neutral and Plasma Distributions in the Coma of Comet C/2012 S1 ISON: Narrowband Imaging and Integral-Field Spectroscopy

C. A. Schmidt (1,2), R. E. Johnson (1), F. Leblanc (2) J. Baumgardner (3) and M. Mendillo (3) (1) University of Virginia, Charlottesville, VA USA (2) Laboratoire Atmosphères, Milieux, Observations Spatiales, IPSL, CNRS, UPMC, Paris, France (3) Boston University, Boston, MA USA (carl.schmidt@virginia.edu)

Abstract

We present concurrent spectra and filtered imaging of the coma of C/2012 S1 ISON at .44 to 0.47 AU from the sun. C_2, NH_2, Na, and H_2O^+ distributions were elongated several thousand km along an axis perpendicular to the comet's motion and the sunward vector. The peak brightness of each species was collocated within 5,000 km of the dusty continuum concentration. ISON's water ion tail appeared distinctly broader than the neutral Na tail and we find no evidence for an extended source of Na by dissociative recombination of a molecular ion. Rather, an extended source of as much as 50% of Na may be attributed to dust, evidenced via Monte Carlo simulations of a distant sodium tail extending beyond 10^6 km. An increase of nearly a factor of four in the Na source rate was found within a 24 hour interval during an outburst, and the relative Na/O abundance is estimated at ~5 x 10^{-7}, well below the ratio known in active comets of comparable geometry.

1. Introduction

Comet C/2012 S1 ISON survived just 14 months between discovery and disintegration just prior to its 2.7 R_{Sun} perihelion. The highly varied water production was monitored using a Lyman α proxy with a source rate as high as 1.1 x 10^{30} s^{-1} during these observations [1]. Fragmentation of the nucleus likely occurred at 0.65 AU from the Sun, with further breakup subsequently and frequent outbursts along its inbound trajectory. A close passage to the Earth (0.86 AU) with near 90° phase angles gave ideal conditions for mapping gas distributions in the coma of this bright, active and pristine Oort cloud comet. We used this opportunity to optimize spatial resolution of the neutral, plasma and dust distribution of the coma.

2. Methods

ISON was observed from McDonald Observatory in Fort Davis, TX, with two small co-aligned optical telescopes on 19.5 and 20.5 Nov 2013. A 40 cm Cassegrain feeding an image-slicer spectrograph (R~20,000) is used here to measure C_2, NH_2, Na, and H_2O^+ emission lines in comet coma within a narrow spectral window spanning 5868Å to 5926Å. The spatial distributions of these species are mapped over a 1.6 x 2.7 arc-minute field made up of 240 individual spectra. Monochromatic images are assembled from individual emission lines, selected to minimize blending in overlapping spectral features. These images are grouped by species, shifted to a common optocenter centroid and co-added to yield distributions in the coma on scales of 10^4 km. At these distances from the nucleus, neutral molecules can be approximately modeled using a Haser analytic formula, while other species demand a more complex treatment.

On larger 10^6 km scales, a small 10 cm refracting telescope with a 7° wide field isolated Na emission by differencing narrowband (14Å) filters centered at 5893Å and 6051Å. In this large field, background spectral standard stars provided an absolute flux calibration through high airmass observing angles. At these distances from the nucleus, the Na tail can be simulated using ballistic atomic trajectories ejected from a collisional radius analogous to a planet's exobase with Monte Carlo seeding. This method integrates the 3D equation of motion of 10^6 particles, considering the effects of gravity, radiation pressure and photo-ionization using a high-resolution solar spectrum interpolated from Earth orbit.

3. Results

ISON's dust distribution fell off less steeply than the canonical inverse with distance from the nucleus and C_2 and NH_2 scale lengths indicate an extended source, possibly due to nucleus fragmentation. No evidence of prompt Triplet or Asundi emissions from CO_2 dissociation into CO is found. The Na tail appears distinctly wider than the ion tail, evidencing dust as the extended source rather than a parent molecular ion (e.g., $NaCl^+$ is known to populate atomic Na clouds from the Io plasma torus). The Na D2/D1 ratio is everywhere 1.38 $\pm$ .10 despite being optically thin.

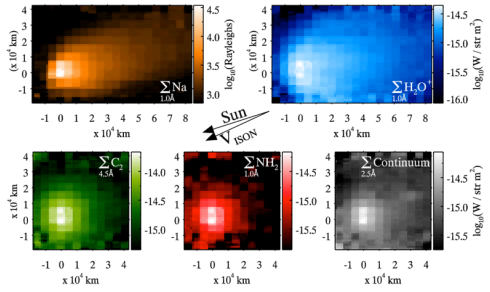

Figure 1: Spatial reconstructions of Na, H_2O^+, C_2, NH_2 and dusty continuum on 20.5 November 2013.

On UT 19.5 Nov 2013, the distant Na tail can be reproduced by 1.6$\pm$0.3 x 10^{23} atoms s^{-1} with nearly half of this production attributed to an extended source such as dust grains. Na production increased to 5.8 $\pm$ 1 x 10^{23} atoms s^{-1} during the following 24 hours, 85% of this within 12,000 km of the nucleus. After this outburst, production became ~5 x 10^{-7} that of water, well below the relative abundance determined in active comets of comparable geometry [2].

4. Summary and Conclusions

We reconstruct the spatial distributions of Na, H_2O^+, C_2, NH_2 and dust in the coma of C/2012 S1 ISON using high-resolution integral-field spectroscopy and differenced narrowband imaging. These data show a very low relative abundance of Na in ISON's coma with a rapidly variable production rate. Consistent with observations of Halley and Hale-Bopp, an extended source is important in the structure of sodium in ISON's coma. These results effectively rule out the possibility of a long-lived ionic parent and strongly suggest dusty origins as an extended source of neutral sodium.

Acknowledgements

We thank the director and staff at McDonald Observatory for their continued support and assistance with measurements from the Boston University station.

References

[1] Combi, M.R., Fougere, N., Mäkinen, J.T.T., Bertaux, J.-L., Quémerais, E., Ferron, S.: Unusual water production activity of Comet C/2012 S1 (ISON): Outbursts and continuous fragmentation. Astrophys. J. 788 (1), L7, 5pp. 2014.

[2] Schmidt, C.A., Johnson, R.E., Baumgardner, J., Mendillo, M.: Observations of sodium in the coma of Comet C/2012 S1 (ISON) during outburst. Icarus, 247 313–318, 2015.

EPSC Abstracts
Vol. 10, EPSC2015-486, 2015
European Planetary Science Congress 2015

A molecular survey of comet C/2014 Q2 (Lovejoy) at radio wavelengths

N. Biver (1), R. Moreno (1), J. Boissier (2), D.C. Lis (3), D. Bockelée-Morvan (1), J. Crovisier (1), P. Colom (1), G. Paubert (4), S. Milam (5), Aa. Sandqvist (6), A. Hjalmarson (7), S. Lundin (8), T. Karlsson (8), M. Battelino (8), U. Frisk (9), D. Murtagh (10), L. Nordh (11) and the Odin team.
(1) LESIA, Observatoire de Paris, CNRS, UPMC, Université Paris-Diderot, 5 place Jules Janssen, F-92195 Meudon, France, (nicolas.biver@obspm.fr); (2) IRAM, 300, rue de la Piscine, F-38406 Saint Martin d'Hères, France; (3) LERMA, Observatoire de Paris, PSL Research University, CNRS, Sorbonne Universités, UPMC Univ. Paris 06, 61 av. de l'Observatoire, F-75014, Paris, France; (4) IRAM, Avd. Divina Pastora, 7, 18012 Granada, Spain; (5) NASA Goddard Space Flight Center, Astrochemistry Laboratory, Code 691.0, Washington, USA; (6) Stockholm Observatory, AlbaNova University Center, SE-106 91 Stockholm, Sweden; (7) Onsala Space Observatory, Chalmers University of Technology, SE-439 92 ONSALA, Sweden; (8) OHB Sweden, P.O. Box 1269, SE-164 29 Kista, Sweden; (9) Omnisys Instruments, August Barks Gata 6B, SE-421 32 Västra Frölunda, Sweden; (10) Dept. of Radio and Space Science, Chalmers Technical University, Gothenburg, Sweden; (11) Swedish National Space Board, Box 4006, SE-171 04 Solna, Sweden

Abstract

Comet C/2014 Q2 (Lovejoy) is a long period Oort Cloud comet (original orbital period = 11030 years, inclination = 80.3°) which passed perihelion at 1.290 AU from the Sun on 30 January 2015. It brightened very quickly as it approached the Sun and the Earth (perigee at 0.469 AU on 7 January 2015) to reach naked eye visibility (m1 = 4) and a total production rate approaching $Q_{H_2O} = 10^{30}$ molec.s^{-1}.

This comet was intrinsically the most active comet since C/1995 O1 (Hale-Bopp) and we triggered target-of-opportunity observations with the IRAM-30m, NOEMA, ALMA, CSO, Nançay and Odin radiotelescopes. The water outgassing was monitored via observations of the OH radical at 18-cm with the Nançay radiotelescope from December to March 2015. Observations of H_2O and $H_2^{18}O$ with the Odin submillimeter space telescope were carried out between 30 January and 03 February.

The comet was observed with the IRAM-30m radiotelescope in Spain on January 13.8, 15.8 and 16.8, with some complementary observations on January 23.7, 24.7, 25.7 and 26.7 under good weather. One objective was to support the ALMA program 2013.1.00686.T (PI S. Milam). It was also observed with NOEMA (25.8 and 28.8 January, PI J. Boissier) and shortly with CSO on February 13.3 and 16.3 UT.

We will present here the analysis of the IRAM data set, which is the most sensitive survey of the molecular content of a comet ever obtained since comet Hale-Bopp. We covered ≈48 GHz of the 1mm band (Fig.1) enabling the detection of over 20 molecules plus radicals and isotopologues.

We will present the measured molecular abundances and sensitive upper limits obtained on a number of complex molecules and of particular (prebiotic) interest. The comet seems relatively depleted in organic molecules compared to our sample of comets investigated at submillimeter wavelengths ([6, 1, 2, 3, 4, 5]).

Acknowledgements
IRAM is supported by INSU/CNRS (France), MPG (Germany) and IGN (Spain). Odin is a Swedish-led satellite project funded jointly by the Swedish National Space Board (SNSB), the Canadian Space Agency (CSA), the National Technology Agency of Finland (Tekes) and the Centre National d'Études Spatiales (CNES, France). The Swedish Space Corporation is the prime contractor, also responsible for Odin operations

References

[1] Biver, N., Bockelée-Morvan, D., Crovisier, J., et al. 2006, *Astron. Astrophys.*, 449, 1255
[2] Biver, N., Bockelée-Morvan, D., Colom, P., et al., 2011, *Astron. Astrophys.*, 528, A142
[3] Biver, N., Bockelée-Morvan, D., Crovisier, J., et al. 2014, *Astron. Astrophys.*, 566, L5
[4] Biver, N., Agundez, M., Milam. S., et al., 2014, 46B Asteroids, Comets, Meteors 2014. Helsinki, Finland.
[5] Biver, N., Bockelée-Morvan, D., Debout, V., et al., 2014, 45B Asteroids, Comets, Meteors 2014. Helsinki, Finland.
[6] Crovisier, J., Biver, N., Bockelée-Morvan, D., et al. 2009 Earth, Moon, and Planets, 105, 2-4, 267–272

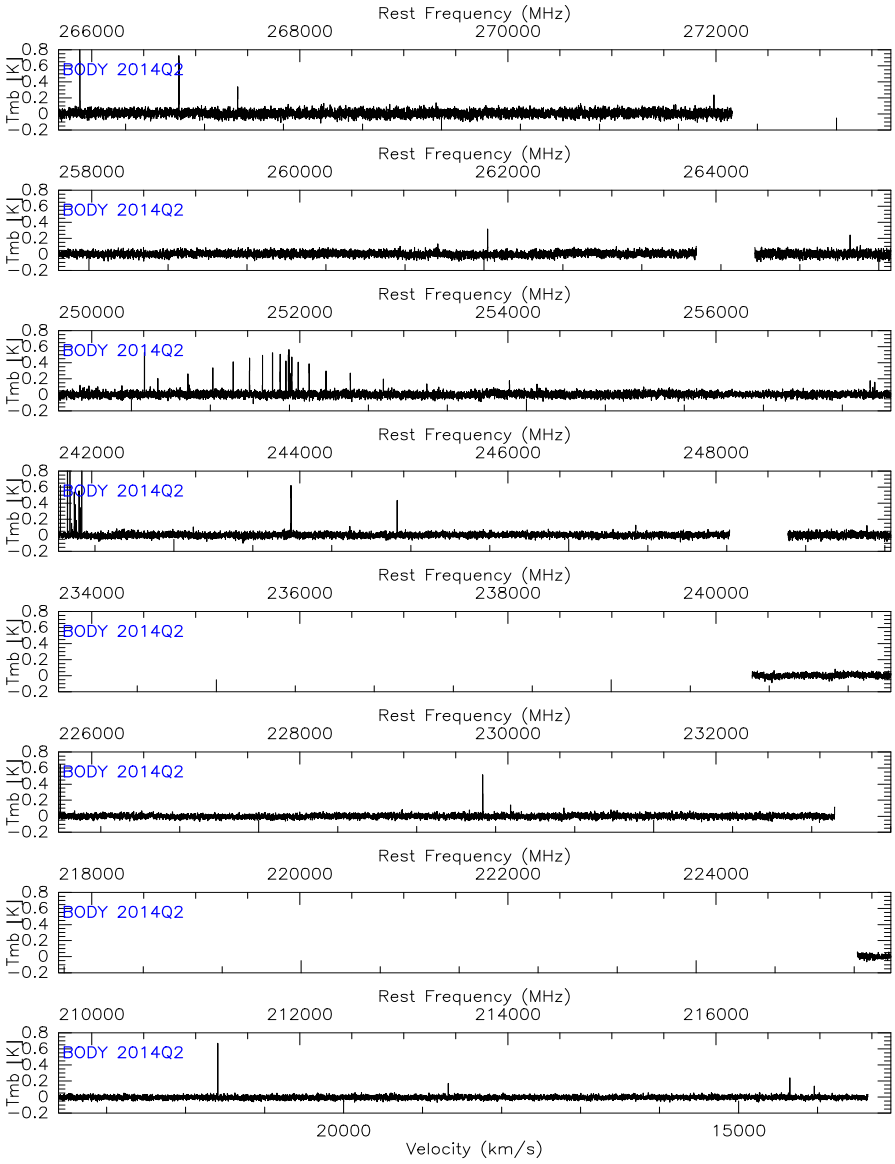

Figure 1: Spectra of comet C/2014 Q2 (Lovejoy) obtained on 13.8 January 2015 with the IRAM-30m.

EPSC Abstracts
Vol. 10, EPSC2015-495, 2015
European Planetary Science Congress 2015

Compaction of ice pebbles in collapsing pebble clouds and the dust-to-ice ratio of comets

S. Lorek (1), B. Gundlach (2), P. Lacerda (1), and J. Blum (2)
(1) Max-Planck Institute for Solar System Research, Justus-von-Liebig-Weg 3, D-37077 Göttingen, (2) Institute for Geophysics and Extraterrestrial Physics, Technische Universität Braunschweig, Mendelssohnstr. 3, D-38106 Braunschweig (lorek@mps.mpg.de)

Abstract

The gravitational collapse of pebble clouds formed in the streaming instability provides a mechanism for comet formation, which agrees well with the observed properties of comets, such as their low density. We numerically investigated the collapse of an ensemble of porous ice and silica pebbles and studied the final filling factor of these pebbles. Based on these results, we estimated the dust-to-ice ratio of the cometesimal and its dependency on initial conditions.

1 Introduction

Comets are believed to have formed as icy planetesimals from dust and ice grains beyond the ice line in the Solar Nebula about $4.5\,\mathrm{Gyr}$ ago. However, growth from μm-sized particles to km-sized bodies is difficult because bouncing [10] and fragmentation [1, 4] stall growth. The streaming instability circumvents those growth barriers by strongly concentrating dust and ice pebbles, leading to the formation of gravitationally bound clumps, which can collapse into a solid object, such as a cometesimal [6, 8].

Cometary densities are low ($\sim 0.4\,\mathrm{g\,cm^{-3}}$). Collapsing pebble clouds are a suitable environment to explain this [2, 3, 7]. Low-velocity bouncing collisions during the collapse yield a body with a pebble packing fraction of $\phi_\mathrm{p} \approx 0.6$. Additionally, dust growth in the Solar Nebula produces pebbles with a filling factor of $\phi \approx 0.4$ [10]. Thus, the total filling factor of the comet is $\phi_\mathrm{c} = \phi_\mathrm{p} \times \phi = 0.24$, in agreement with the observed low density [7].

2 Method

We conducted numerical simulations of collapsing pebble clouds with a pre-existing Monte Carlo method [9, 8] and followed the evolution of the volume filling factor of the pebbles. We adapted the collision model for porosity and water ice by scaling the threshold velocities for sticking, bouncing, and fragmentation, and the compression curve of ice by a factor of ten [5].

In our study, we used $1\,\mathrm{cm}$ pebbles with varying initial filling factor, ϕ_0, from 0.001 (very porous) to 0.4 (compact). We investigated three cloud masses corresponding to a $5\,\mathrm{km}$ (low-mass), a $50\,\mathrm{km}$ (intermediate-mass), and a $500\,\mathrm{km}$ (high-mass) object with a bulk density of $0.4\,\mathrm{g\,cm^{-3}}$. We simulated the collapse of ice and silica pebbles separately and used the results to derive a dust-to-ice ratio, ξ, for the cometesimal.

3 Results

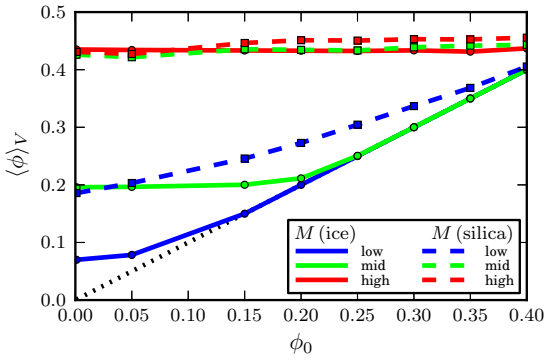

Figure 1: Pebble compaction. Final filling factor of the pebbles as a function of their initial filling factor. Different coloured lines correspond to different pebble cloud masses. Solid lines correspond to ice pebbles and dashed lines to silica pebbles. Along the black dotted line, the final filling factor equals the initial filling factor.

Our simulations showed that silica pebbles are sig-

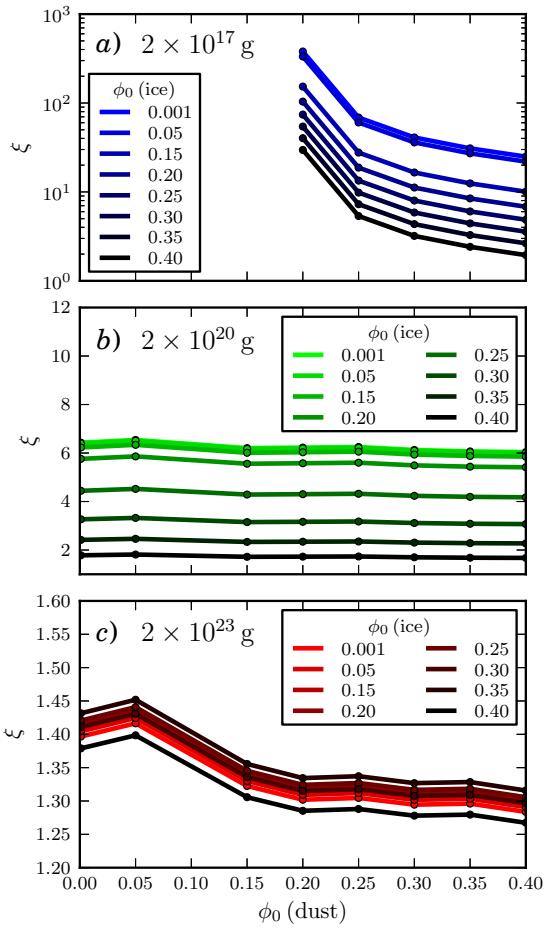

Figure 2: Dust-to-ice ratio, ξ, of the comet as a function of initial filling factor of the pebbles. *a*) low-mass cloud; *b*) intermediate-mass cloud; and *c*) high-mass cloud.

nificantly compressed during the collapse acquiring a filling factor of $\phi \approx 0.19 - 0.45$ (Fig. 1). In contrast, ice pebbles are barely compressed and retain their initial filling factors, unless the cloud is massive (Fig. 1). Thus, the dust-to-ice ratio varies strongly with initial conditions taking values between 380 and 1.3 (Fig. 2). Starting with compact ($\phi_0 = 0.4$) ice and dust pebbles in the low-mass cloud, the dust-to-ice ratio is about 2. ξ is insensitive to ϕ_0 of the silica pebbles in the intermediate- and high-mass case. In the high-mass case, the dust-to-ice ratio is also insensitive to ϕ_0 of ice.

4 Conclusion

We found that silica pebbles are significantly compressed during the collapse of a pebble cloud, whereas ice pebbles retain most of their initial porosity because of their ten times higher compression strength. Thus, the dust-to-ice ratio of a comet required to account for the low density varies strongly with initial conditions. If both ice and silica pebbles posses an initial filling factor of 0.4 in the low-mass cloud, the dust-to-ice ratio takes a value of ~ 2. For the intermediate- and high-mass cloud, the dust-to-ice ratio is insensitive to the initial filling factor of the silica pebbles. In the high-mass case, also the initial porosity of the ice pebbles does not play any role.

Acknowledgements

S. L. would like to thank Karl Wahlberg Jansson for discussion and pointing out a missing factor of two.

References

[1] Blum, J. and Wurm 2008, G., ARA&A, 46, 21-56

[2] Blum, J. et al. 2014, Icarus, 235, 156-169

[3] Blum, J. et al. 2015, Icarus, 248, 135-136

[4] Güttler et al. 2010, A&A, 513, A56

[5] Gundlach, B. and Blum, J. 2015, Icarus, 214, 717-723

[6] Johansen, A. et al. 2007, Nature, 448, 1022-1025

[7] Skorov, Y. and Blum, J. 2012, Icarus, 221, 1-11

[8] Wahlberg Jansson, K. and Johansen, A. 2014, A&A, 570, A47

[9] Zsom, A. and Dullemond, C. P. 2008, A&A, 489, 931-941

[10] Zsom A. et al. 2010, A&A, 513, A57

EPSC Abstracts
Vol. 10, EPSC2015-498, 2015
European Planetary Science Congress 2015

Scenarios for distributed sources of formaldehyde in the atmosphere of comet 67P/Churyumov-Gerasimenko

H. Cottin (1), K. Hadraoui (1), A. Bardyn (1,2), L. Le Roy (3), N. Fray (1), C. Briois (2), L. Thirkell (2), S. Merouane (4), K. Hornung (5), Y. Langevin (5), M. Hilchenbach (4) AND THE COSIMA TEAM

(1) Laboratoire Interuniversitaire des Systèmes Atmosphériques, LISA, UMR CNRS 7583, Université Paris Est Créteil et Université Paris Diderot, Institut Pierre Simon Laplace, France

(2) Laboratoire de Physique et Chimie de l'Environnement et de l'Espace, CNRS / Université d'Orléans, 3 Av. de la Recherche Scientifique, 45071 Orléans, France

(3) Center for Space and Habitability (CSH), University of Bern, Sidlerstrasse 5, 3012 Bern, Switzerland

(4) Max-Planck-Institut für Sonnensystemforschung, Justus-von-Liebig-Weg 3, 37077 Göttingen, Germany

(5) Universität der Bundeswehr LRT-7, Werner Heisenberg Weg 39, 85577 Neubiberg, Germany

(6) Institut d'Astrophysique Spatiale, CNRS / Université Paris Sud, Bâtiment 121, 91405 Orsay

(herve.cottin@lisa.u-pec.fr / Fax: +33-no-one-use-faxanymore)

Abstract

The polymer of formaldehyde ($(H_2CO)_n$ - polyoxymethylene – POM) has been tentatively detected in comet 1P/Halley by mass spectrometry with PICCA instrument onboard the Giotto spacecraft [1]. Although its detection has been questioned [2], this polymer could be the origin of distributed formaldehyde observed in the atmosphere of comet Halley and others [3]. We will present modelling results of the photo and thermal degradation of POM on grains in the environment of comet 67P/Churyumov-Gerasimenko, and discuss the extent to which distributed formaldehyde could be detected with Rosetta spacecraft observations in case POM is actually part of the nucleus component.

1. Distributed sources of formaldehyde in comets

Formaldehyde (H_2CO) observations in comets 1P/Halley [4], C/1995 O1 (Hale-Bopp) [5], C/2012 F6 (Lemmon) and C/2012 S1 (ISON) [6] are consistent with a distributed source for this molecule in there atmospheres. This means that H_2CO cannot only be released from the nucleus of the comets, but rather from a parent compound that could not be identified in the gaseous phase. Thanks to proper modelling based on experimental measurements in the laboratory [7] [8], it has been shown in the case of comets 1P/Halley [9] (see Figure 1) and C/1995 O1 (Hale-Bopp) [10] that the presence of polyoxymethylene in the solid phase at the percent level in grains, and its photo & thermal degradation throughout the atmosphere of the two comets, could account for the observed distribution density of H_2CO.

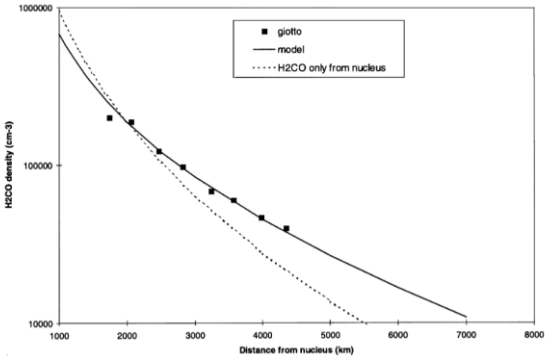

Figure 1: Formaldehyde density profile in comet Halley measured by Giotto (squares) and calculated with (continuous line) or without (dotted line) distributed production of H2CO from POM. Figure from [11]

2. Scenarios for distributed H_2CO from POM comet 67P/Churyumov-Gerasimenko

Taking into account the grain size distribution as measured by the COSIMA instrument onboard the ROSETTA spacecraft [12], and the actual activity of the comet, we have studied the extent to which formaldehyde could show a significant distributed source of formaldehyde in the atmosphere of comet 67P if polyoxymethylene is part of the grain component. We will discuss trajectories of the spacecraft and observations that could tell whether formaldehyde is distributed or not.

References

1. Huebner, W.F., *First polymer in space identified in comet Halley.* Science, 1987. **237**(August): p. 628-630.
2. Mitchell, D.L., et al., *The origin of complex organic ions in the coma of comet Halley.* Icarus, 1992. **98**: p. 125-133.
3. Cottin, H. and N. Fray, *Distributed Sources in Comets.* Space Science Reviews, 2008. **138** (1-4): p. 179-197
4. Meier, R., et al., *The extended formaldehyde source in comet P/Halley.* Astronomy and Astrophysics, 1993. **277**: p. 677-691.
5. Biver, N., et al., *The 1995-2002 Long-Term Monitoring of Comet C/1995 O1 (HALE-BOPP) at Radio Wavelength.* Earth Moon and Planets, 2002. **90**: p. 5-14.
6. Cordiner, M.A., et al., *Mapping the Release of Volatiles in the Inner Comae of Comets C/2012 F6 (Lemmon) and C/2012 S1 (ISON) Using the Atacama Large Millimeter/Submillimeter Array.* The Astrophysical Journal Letters, 2014. **792**(1): p. L2.
7. Cottin, H., et al., *An experimental study of the photodegradation of polyoxymethylene at 122, 147 and 193 nm.* Journal of photochemistry and photobiology, 2000. **135**(A : Chemistry): p. 53-64.
8. Fray, N., et al., *New experimental results on the degradation of polyoxymethylene. Application to the origin of the formaldehyde extended source in comets.* Journal of Geophysical Research (Planets), 2004. **109**: p. E07S12.
9. Cottin, H., et al., *Origin of cometary extended sources from degradation of refractory organics on grains: polyoxymethylene as formaldehyde parent molecule.* Icarus, 2004. **167**: p. 397–416.
10. Fray, N., et al., *Heliocentric evolution of the degradation of polyoxylmethylene. Application to the origin of the formaldehyde (H2CO) extended source in comet C/1995 O1 (Hale-Bopp).* Icarus, 2006. **184**(1): p. 239-254.
11. Cottin, H., et al., *Polyoxymethylene as parent molecule for the formaldehyde extended source in comet Halley.* The Astrophysical Journal, 2001. **556**(1): p. 417-420.
12. Kissel, J., et al., *COSIMA, a High Resolution Time of Flight Spectrometer for Secondary Ion Mass Spectroscopy of Cometary Dust Particles.* Space Science Reviews, 2007. **128**(1-4): p. 823-867.

EPSC Abstracts
Vol. 10, EPSC2015-549, 2015
European Planetary Science Congress 2015

Analysis of H_2O rotational lines in comets with the *Herschel* PACS observations

A. Decock (1), D. Bockelée-Morvan (1), N. Biver (1), E. Lellouch (1), B. Vandenbussche (2), and P. Hartogh (3)
(1) LESIA, Observatoire de Paris, Meudon, France (alice.decock@obspm.fr), (2) Institute for Astronomy, KU, Leuven, Belgium, (3) Max-Planck-Institut für Sonnensystemforschung, Katlenburg-Lindau, Germany

1. Introduction

Comets are among the best preserved specimens of the primitive solar nebula. Analyzing molecular components in comets could thereby provide information on the formation and evolution of our Solar System [1]. It is important to study the molecules in comets of various origins as they might come from various parts of the accretion disk and the species might have been formed under various chemical and physical conditions. Water constitutes usually 80% of cometary ices. Studying this molecule is thus essential to determine the nature of comets and characterize the molecular composition of them.

2. Observations and analysis of water lines

An accurate measurement of H_2O in comets from observations of its rotational lines is not easy because H_2O lines are often optically thick. The *Herschel Space Observatory* and its Photodetector Array Camera and Spectrometer (PACS) are well suited to search and analyze the water lines. We report observations carried out as a part of the "Water and related chemistry in the Solar System" guaranteed time key program for *Herschel* [2]. The PACS spectroscopic observations cover the spectrum between 55 and 220μm in four scans: two using the blue detector array (50-70μm and 70-100μm) and two using the red dectector array (100-150μm and 130-220μm).

We analyzed the PACS data of the comets 10P/Tempel 2, 103P/Hartley 2, 45P/Honda-Mrkos-Pajdusakova and C/2009 P1 (Garradd) in order to study the H_2O lines and search for $H_2^{18}O$ lines. Our data sample is really interesting because it contains not only Oort Cloud comets (OCC) but also Jupiter Family comets (JFC) and all the spectra were acquired with the same instrumentation. An example of a reduced spectrum obtained with PACS is presented in

Figure 1.

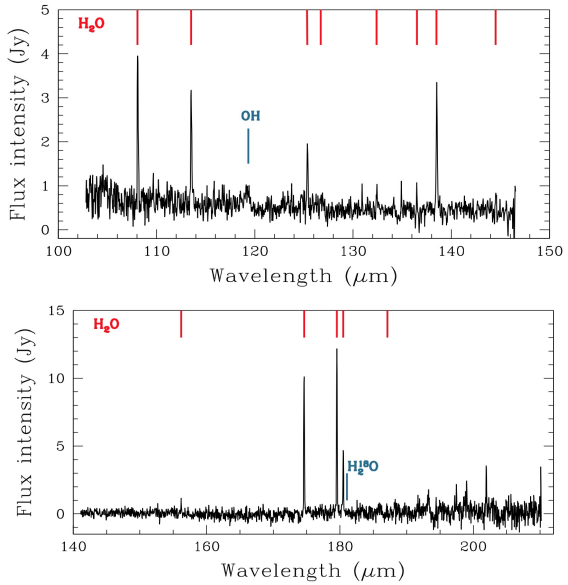

Figure 1: Two wavelength ranges of a spectrum of 103P/Hartley 2 obtained on 11 Nov 2010 with PACS instrument. Identified H_2O lines are indicated with red ticks. Bottom: Detected $H_2^{18}O$ line is pointed with a blue tick.

This work is based on excitation and radiation transfer models of H_2O and $H_2^{18}O$ provided by Biver et al. [3] but a preliminary examination of the relative intensities of lines at 179.5 and 180.5 μm and their brightness distribution suggest that these models need to be improved. We thus made a joint analysis of fifty observed water lines in order to identify the sources of disagreements. The interpretation of the spectral data also required to carefully take into account the PACS point spread function (PSF). Since the radiative transfer models include physical processes affecting the excitation of molecules, one of the main goals

of this analysis aims in a better understanding of the excitation mechanisms of water. Refining the models could then better constrain the water distribution and the water production rate in comets.

Acknowledgements

Herschel is an ESA space observatory with science instruments provided by European-led Principal Investigator consortia and with important participation from NASA. PACS instrument has been developed by a consortium of institutes led by MPE (Germany) and including UVIE (Austria); KU Leuven, CSL, IMEC (Belgium); CEA, LAM (France); MPIA (Germany); INAF- IFSI/OAA/OAP/OAT, LENS, SISSA (Italy); IAC (Spain). This development has been supported by the funding agencies BMVIT (Austria), ESA-PRODEX (Belgium), CEA/CNES (France), DLR (Germany), ASI/INAF (Italy), and CICYT/MCYT (Spain).
A. Decock acknowledges the support of the DIM ACAV post-doctoral grant.

References

[1] Ehrenfreund, P., & Charnley, S. B.: A&A, 38, 427, 2000.

[2] Hartogh, P., Lellouch, E., Crovisier, J., et al.: Planetary Space Science, 57, 1596, 2009.

[3] Biver, N., Bockelée-Morvan, D., Crovisier, J., Lecacheux, A., Frisk, U., Hjalmarson, Å., Olberg, M., Florén, H.-G., Sandqvist, A. & Kwok, S., Planetary and Space Science, 55, 9, 1058-1068, 2007.

EPSC Abstracts
Vol. 10, EPSC2015-592, 2015
European Planetary Science Congress 2015

Re-analysis of the Giotto mission data obtained by the Halley Multicolour Camera (HMC) with aim of large particles detection in the inner coma of comet 1P/Halley

O. S. Shalygina, H. U. Keller and J. Blum
Technische Universität Braunschweig, Institute for Geophysics and Extraterrestrial Physics (IGEP), Braunschweig, Germany (o.shalygina@tu-braunschweig.de)

1. Giotto mission and HMC

The Giotto spacecraft (SC) mission was the ESA's first interplanetary mission, that made close-up observations of a comet. The Giotto spaceprobe passed the nucleus of comet Halley at a fly-by distance of only 596 km early on 14 March 1986. During the approach, 2304 images of the comet were taken by the Halley Multicolour Camera (HMC) through different filters.

The HMC experiment was a high-resolution imaging system onboard the spin-stabilized SC. Its spin axis was closely aligned with the SC-comet relative-velocity vector. Pointing of the camera was achieved by the spinning motion of the SC for one dimension and by rotation about an axis perpendicular to the spin of the SC for the other dimension. The spin period was about 4 seconds and the nominal imaging resolution was 22 m at 1000 km distance [1, 2].

HMC was taking images in the so-called Time Delay and Integration mode [2]. In this mode, only a narrow part of the CCD detector was uncovered, and vertical scan-out was provided by the spacecraft (and therefore the camera) spinning. During this spinning charges were transferred line-by-line in the same direction. The slit was made wider than 1 pixel, which increased exposure time but degraded the sharpness to some extent. The portion of the sky swept by the exposed lines during image acquisition was a section of an annulus resulting in over-sampling at the end of the exposed lines nearest the SC spin axis and under-sampling at the other end [2].

Several impacts of dust particles on the spacecraft were detected during the fly-by by the analysis of the changes in the SC attitude and spin period [1]. The changes occurred in large steps, requiring many impacts of massive dust particles well above an effective mass of 10 mg, which implies that a significant part of the cometary dust mass is contained in rather large particles. Moreover, since the time of the Giotto mission, large dust particles have been detected in the inner coma of other comets. The coma of comet 103P/Hartley 2 has a significant population of large particles observed as point sources in images taken by the Deep Impact SC, with particle radii extending up to 20 cm, and perhaps up to 2 m (dependent on the assumed albedo) [3]. So, it is worthwhile re-analyzing the HMC data for large-particles detection at HMC images.

2. Detectability of large particles by HMC

Before searching the particles in the HMC images, it is required to estimate ability of the HMC to detect such particles at all. The minimum detectable particle radii depend on their light scattering properties. Our estimations show that dusty particles with radii of about 1 m to 1.5 m and larger can be detected at the closest approach (in case of high-albedo icy particles, the size decreases to centimeters). These obtained values are in accordance with the estimations made for comet 103P/Hartley 2 [3].

Our estimations show that particles near the nucleus (distance from the camera to particle $\sim 10^3$ km) may be detected even if they are moving quite fast, but for the particles that are ten times closer to the camera (100 km) tangential speed of kilometres per second significantly decreases detection possibility.

If the ejected particle moves directly to the place where the HMC is at the time of observations, it can become more visible for the camera. If a particle moves with a speed of at least $10\,\mathrm{m\,s^{-1}}$, it can easily travel tens of thousand kilometers in three months (approximate time from the start of the nucleus activity to the HMC observations in March 1986).

According to our estimations of particle detectability, a set of images with numbers from 3436 to 3493 (distances from camera to nucleus are in the range of 20 000 km to 4000 km) was selected to search for the evidence of large particles.

3. Searching for the large particles

It is not sufficient to analyse the consecutive images by the image-differencing method. To distinguish between dust particles and sporadic noise in the images, space coherence of the former may be used. Thus, precise boresight vectors are a crucial part of the particle detection method. Positions of moving particles at subsequent times must form straight lines with an origin at the nucleus. What we expect from the algorithm is the confident detection of all pixels that contain probable images of a dust particle, which stays or moves with arbitrary speed along a straight line in space.

Our particle-detection algorithm consists of three main blocks:

- Detection of suspicious pixels (whose brightness significantly differs from that of surrounding pixels) in images.
- Finding all possible trajectories that can produce these pixels.
- Validating the derived trajectories: the valid ones have to start at the nucleus, the velocity of the particle along the trajectory has to stay constant within reasonable limits, and trajectory intersections with the boresight vectors have to be in the correct order.

A detailed description of the particle-detection algorithm, its implementation and optimization, as well as the results from our analysis of HMC images will be presented.

Acknowledgements

This study is supported by European Space Agency grant no. 4000109609/13/NL/JK. We are grateful to the staff of the Max-Planck-Institut für Sonnensystemforschung (Göttingen, Germany), namely to U. Mall, I. Pardowitz and H. Michels, for their help with HMC data conversion, and to J. Kramm and W. Curdt for the consultations and productive discussions.

References

[1] W. Curdt and H. U. Keller. “Large dust particles along the Giotto trajectory”. In: *Icarus* 86.1 (1990), pp. 305–313.

[2] H. U. Keller, W. Curdt, et al. *Images of the Nucleus of Comet Halley obtained by the Halley Multicolour Camera (HMC) on board the Giotto spacecraft*. Ed. by R. Reinhard, N. Longdon, et al. Vol. 1. Atlas of Images the Nucleus of Comet Halley. ESTEC, Nordwijk, The Netherlands: ESA Publications Division, 1994.

[3] M. S. Kelley, D. J. Lindler, et al. “A distribution of large particles in the coma of Comet 103P/Hartley 2”. In: *Icarus* 222.2 (2013), pp. 634–652.

EPSC Abstracts
Vol. 10, EPSC2015-627, 2015
European Planetary Science Congress 2015

Dynamical simulations of cometary dust within the near-nucleus environment

Yu. Skorov, P. Lacerda
(1) Max Planck Institute for Solar System Research, Göttingen, Germany (skorov@mps.mpg.de)

Abstract

The Rosetta mission to comet 67P/Churyumov-Gerasimenko is providing unique constraints on the physical and dynamical properties of cometary dust (Rotundi et al. 2015, Schultz et al. 2015), and some of the first results are surprising. Examples include:

- Very large dust grains were detected near the nucleus at heliocentric distances greater than 3.5 AU. Grains from about ten to several hundred micron in size have been detected and collected by GIADA and COSIMA, while the OSIRIS camera revealed tracks of particles up to 2 cm in diameter;
- Dust grains from 67P hit the detectors at speeds 1 to 10 m/s, and grain speed is not strongly correlated with size. Optically detected grains move away from the nucleus at around 3.5 m/s;
- The dust grains appear to be weakly bound, fluffy agglomerates with porosities about 50%.

These results have motivated us to reassess the complex dynamics of cometary dust in the relatively unconstrained near-nucleus region. Here we present models of idealised dust particles and simulate their interactions with gravity from the sun and the nucleus, with solar radiation, and with sublimating gas drag. The dust particles are modelled as porous random aggregates constructed using different algorithms: ballistic particle-cluster aggregation (BPCA, or BA for short), ballistic agglomeration with one migration (BAM1), ballistic agglomeration with two migrations (BAM2), hierarchical aggregates of aggregates (AgAg) and ballistic cluster-cluster aggregates (BCCA).

1. Model Details

Following [3], we model dust grains as random aggregates of monomers with a wide range of filling factors, from 0.15 for BA aggregates, where incoming monomers stick to the growing cluster at the first point of contact, to 0.30 for BAM2 aggregates, where incoming monomers are allowed up to two migrations before sticking.

In addition, we consider for the first time hierarchical aggregates (AgAg, see [4]). Hierarchical aggregates have a spatial structure similar to that of the well-known BCCA aggregates, which are also considered in our study.

Radiative forces are calculated following [5], and the optical properties of the particles are calculated using a combination of Mie theory and effective medium theory. Forces due to gas drag account for the non-equilibrium velocity distribution of gas molecules [6]. A mean momentum transfer from a gas molecule to the aggregate is estimated by Monte-Carlo simulations.

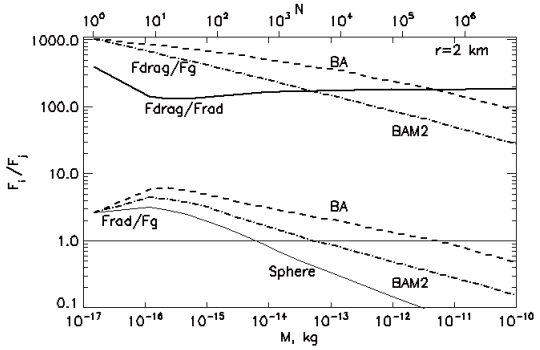

Figure 1: Ratio of different forces acting on grains: F_{drag}/F_{rad}, F_{drag}/F_g, F_{rad}/F_g, as a function of aggregate mass (or number of monomers) at the surface of a homogeneous spherical nucleus. Results for BA and BAM2 aggregates, and solid spheres are shown.

2. Results

Figure 1 compares the different forces acting on a dust grain near the nucleus surface and shows that gas drag is the dominant force. For all tested particle sizes, gas drag is orders of magnitude larger than cometary gravity and solar radiation forces.

We find that there is maximum size of particle that can be lifted by gas drag, irrespective of the type of aggregate considered. This limit is a function of gas production. If the total gas production of a

homogeneous spherical nucleus is about 2 kg/s the maximum mass of lifted dust grains ranges from 10^{-4} kg for BAM2 aggregates to 10^{-3} kg for BA aggregates. Due to the rapid reduction in the density of the expanding gas, the region of effective dust acceleration is quite small: particles reach terminal speed at a distance of about ten nucleus radii. A dust grain speed is only a few percent of the speed of gas flow, so the gas drag force is decreased mainly due to a decrease in gas density.

3. Conclusions

We find that none of the grains structures considered is able to explain simultaneously 1) the high grain porosity, 2) the low speeds and 3) the "flat" velocity curve of dust grains measured by Rosetta. To explain the latter, we propose that dust grains must break-up well beyond the gas drag acceleration region, and probably near the spacecraft.

References

[1] Rotundi, A. et al. 2015. Dust measurements in the coma of comet 67P/Churyumov-Gerasimenko inbound to the Sun. Science 347, 6220, id. aaa3905.

[2] Schulz, R. et al. 2015. Comet 67P/Churyumov-Gerasimenko sheds dust coat accumulated over the past four years. Nature 518, 216-218.

[3] Shen, Y. et al. 2008. Modeling Porous Dust Grains with Ballistic Aggregates. I. Geometry and Optical Properties. Astroph. J. 689, 260-275.

[4] Skorov, Yu., Blum, J., 2012. Dust release and tensile strength of the non-volatile layer of cometary nuclei. Icarus 221, 1-11.

[5] Kozasa, T., Blum, J., and Mukai, T., 1992. Optical properties of dust aggregates. I - Wavelength dependence. Astron. Astrophys. 263, 423-432.

[6] Skorov, Yu.V., Rickman, H., 1999. Gas flow and dust acceleration in a cometary Knudsen layer. Planet. Space Sci. 47, 935-949

EPSC Abstracts
Vol. 10, EPSC2015-689, 2015
European Planetary Science Congress 2015

Mass loading of the solar wind near comet 67P: a comparison between observations and a hybrid model

E. Behar, M. Holmström, H. Nilsson and G. Stenberg-Wieser
Swedish Institute of Space Physics, Kiruna, Sweden (etienne@irf.se)

Abstract

We compare data from the ion sensor RPC-ICA flying on the european spacecraft Rosetta with results of a hybrid simulation. We study the dynamics of the interaction between the solar wind ions and a partially ionized atmosphere around a comet, further than 2 AU away from the Sun. We discuss how well the model can explain the observations at different heliospheric distances. We also look closely at dynamic changes in the solar wind and the response of the comet ion environment.

Acknowledgements

The work on RPC-ICA, as well as this PhD project, is founded by the Swedish National Space Board. Without the tremendous work of the Rosetta Science Ground Segment (RSGS), Rosetta Mission Operation Control (RMOC) and all instrument team planners, this study would be impossible. Sharing data within RPC is made possible by the web-based interface AMDA, developed and made available for RPC use by Centre de Donnees de la Physique des Plasmas (CDPP). This easy and efficient interface has been of a great use for this work.

References

[1] E. Behar, H. Nilsson and G. Stenberg-Wieser. Mass-loading at 67P/Churyumov-Gerasimenko: a case study. *In preparation*

[2] H. Nilsson, R. Lundin, K. Lundin, S. Barabash, H. Borg, O. Norberg, A. Fedorov, J.-A Sauvaud, H. Koskinen, E. Kallio, P. Riihelä, and J.L. Burch. Rpc-ica: The ion composition analyzer of the rosetta plasma consortium. *Space Science Reviews*, 128(1-4):671–695, 2007.

[3] Hans Nilsson, Gabriella Stenberg Wieser, Etienne Behar, Cyril Simon Wedlund, Herbert Gunell, Masatoshi Yamauchi, Rickard Lundin, Stas Barabash, Martin Wieser, Chris Carr, Emanuele Cupido, James L. Burch, Andrei Fedorov, Jean-AndrÈ Sauvaud, Hannu Koskinen, Esa Kallio, Jean-Pierre Lebreton, Anders Eriksson, Niklas Edberg, Raymond Goldstein, Pierre Henri, Christoph Koenders, Prachet Mokashi, Zoltan Nemeth, Ingo Richter, Karoly Szego, Martin Volwerk, Claire Vallat, and Martin Rubin. Birth of a comet magnetosphere: A spring of water ions. *Science*, 347(6220), 2015.

[4] K. Szegö, K.-H. Glassmeier, R. Bingham, A. Bogdanov, C. Fischer, G. Haerendel, A. Brinca, T. Cravens, E. Dubinin, K. Sauer, L. Fisk, T. Gombosi, N. Schwadron, P. Isenberg, M. Lee, C. Mazelle, E. Möbius, U. Motschmann, V. D. Shapiro, B. Tsurutani, and G. Zank. Physics of Mass Loaded Plasmas. *Space Sci. Rev.*, 94:429–671, December 2000.

EPSC Abstracts
Vol. 10, EPSC2015-711, 2015
European Planetary Science Congress 2015

Energy transfer into the surface layer of 67P/Churyumov-Gerasimenko: constraints on the thermophysical properties from MIRO observations.

Yu. Skorov, P. Hartogh, L. Rezac, C. Jarchow and MIRO team
(1) Max Planck Institute for Solar System Research, Göttingen, Germany (skorov@mps.mpg.de)

Abstract

The thermophysical properties of the surface layer of comets remain surprisingly difficult to assess. The near-absence of pure water ice on the surface implies an ice-free porous dust layer covering a more volatile-rich interior. This hypothesis presents conceptually significant difficulties. These include understanding how dust particles are released from the comet and how heat is transferred to the sub-surface despite the measured (extremely) low thermal inertia.
Our model is designed to place constraints on the thermal, chemical, and structural properties of the surface layer and to establish mechanisms for mass (both volatile and non-volatile) loss as a consequence of these properties. We seek to establish and constrain models of these layers using multiple datasets from the MIRO instrument on board the Rosetta spacecraft.

1. Introduction

The Microwave Instrument for the Rosetta Orbiter (MIRO) performs observations of the nucleus of 67P/Churyumov-Gerasimenko in the millimeter-wave continuum starting from July 2014. The analysis of data obtained at wavelengths of 0.5mm and 1.6mm during August and September 2014 showed that the observed brightness temperatures strongly depend on the diurnal and the seasonal variations of solar illumination. The notable diurnal variations have been detected for the millimeter-wave channel that may be interpreted as the thermal emission from within the region of variable temperature. It means that thermal emission arises at depths of the same order of magnitude as the thermal skin depth. Gulkis et al. (2015) has shown that the observational data are quantitatively consistent with a very low thermal inertia values (~5-30 J K^{-1} m^{-2} $s^{-1/2}$). Such a low thermal inertia clearly shows that the surface region has a high porosity. The effective thermal conductivity of the non-volatile porous layer is a key term in the thermal inertia: only its variations can significantly affect the value of inertia. The resulting estimates suggest that the effective thermal conductivity of the medium is hundreds of times smaller than a typical bulk thermal conductivity. Thus, in addition to the high porosity one should assume that the cometary surface layer is composed of agglomerates which contain micron size particles. Both of these assumptions are supported by the results obtained in other experiments. Dust grains from about ten to several hundred micron in size have been detected and collected by GIADA [2] and COSIMA [3]. The dust grains appeared to be weakly bound, fluffy agglomerates with high porosity.

First qualitative analyses of the data and the first reasoned estimation of thermophysical properties of the uppermost region of the cometary nucleus were obtained using a simple thermal model. However, Schloerb et al (2015 submitted to A&A) noticed that these properties varied not only with the cometocentric position (which may indicate the nucleus inhomogeneity), but also with the depth. They found that the thermal inertia values best fitting the observations of the different channels differ considerably.

These results have motivated us to construct a more detail microscopic model describing energy transfer into the uppermost surface layer in order to get constraints on the thermophysical properties from MIRO observations.

2. Model

MIRO gives us brightness temperatures measured at two unknown depths. Even without detailed informa-

tion about the dielectric properties of the medium we can get some information about the thermophysical properties of the surface layer. The general approach was presented in [5]. The skin depth of the heat wave is very small, resulting in a cometary surface layer which reacts extremely fast to changes in irradiance, so that activity becomes a strongly local property of a surface area. One can therefore expect that the observable effects reflect the distinctions in physical and chemical properties of the nucleus and its inherent heterogeneities.

Recently we suggested a new thermophysical model for cometary nuclei based upon the assumption that comets formed through gravitational instability of an ensemble of dust and ice aggregates [6]. Under this condition, the transport processes as well as the tensile strength of the ice-free outer dust layer were derived. We use available laboratory data of the gas permeability and the thermal conductivity of ice-free porous dust beds. Although this gives our approach a semi-empirical character, we believe that coupling the model to laboratory results puts it on a solid base and is a strong point of our model.

If the characteristic time scales for gas diffusion and heat conduction are smaller than the characteristic time of irradiation changes, the stationary approach to the energy transfer can be applied. In this case in order to evaluate the resulting gas flow and the resulting gas pressure above the sublimating layer one has only to consider energy balances on the top and on the bottom of the refractive porous layer [7]. Thus we get a system of nonlinear equations for temperatures on the surface and on the sublimating front. This system can be effectively solved for the most general case when an effective conductivity is a nonlinear function of temperature. Applying the balance equations for the energy flux at the boundaries of the dust layer one can obtain a similar system of equations for the case when the incoming energy is absorbed in the volume (a so called solid state greenhouse effect) and the thermal radiation is emitted from a non-isothermal porous layer.

A porous refractive layer greatly reduces the effective production for all regimes of gas diffusion (from Knudsen diffusion to a continuous flow). For the collisionless gas flow (Knudsen regime) we use an empirical experimental formula [6]. Three conductivity mechanisms are included into the model: conductivity through a solid medium, conductivity via the thermal emission, and conductivity via the gas diffusion. The detailed description of the model is presented in [7].

3. Conclusions

Based on computer simulations we evaluate the effective thermal inertia of a porous dust medium as a function of its microphysical characteristics. We demonstrate that sublimating ice works as an effective cooler, which decreases the media temperature above the sublimating region. Thus, adding ice to the model we change the general temperature distribution within the surface layer of comet. The ice existence can be recognized in the analysis of MIRO observations. Note that we don't assume that deeper MIRO measurements are related to an icy region, it is enough to assume that such an icy region exists close to the surface. We also accurately evaluate the gas diffusion through the porous dust crust and the effective sublimation rate.

References

[1] Gulkis, S. et al. 2015. Subsurface properties and early activity of comet 67p/churyumovgerasimenko. Science, 347, 6220, id.aaa0709.

[2] Rotundi, A. et al. 2015. Dust measurements in the coma of comet 67P/Churyumov-Gerasimenko inbound to the Sun. Science 347, 6220, id. aaa3905.

[3] Schulz, R. et al. 2015. Comet 67P/Churyumov-Gerasimenko sheds dust coat accumulated over the past four years. Nature 518, 216-218.

[4] Schloerb, F.P. et al. 2015. MIRO Observations of Subsurface Temperatures of the Nucleus of 67P/Churyumov-Gerasimenko. submitted to A&A .

[5] Gundlach, B., Blum, J. 2013. A new method to determine the grain size of planetary regolith, Icarus 223, 479-492.

[6] Skorov, Yu., Blum, J., 2012. Dust release and tensile strength of the non-volatile layer of cometary nuclei. Icarus 221, 1-11.

[7] Keller, H.U. et al. 2015. Insolation, erosion, and morphology of comet 67p/churyumov-gerasimenko. A&A, in press.

EPSC Abstracts
Vol. 10, EPSC2015-806, 2015
European Planetary Science Congress 2015

Observations of the 18-cm lines of the OH radical in comets with the Nançay radio telescope

J. Crovisier, P. Colom, N. Biver, D. Bockelée-Morvan
LESIA, Observatoire de Paris, CNRS, UPMC, Université Paris-Diderot, 5 place Jules Janssen, F-92195 Meudon, France
(jacques.crovisier@obspm.fr)

Since 1973, the 18-cm lines of the OH radical have been systematically observed in selected comets with the 300×40 m radio telescope at Nançay. Up to now, 133 comets have been observed (counting different returns of short-period comets as different comets), totalling about 6000 individual observations (typically one hour per day for each observation).

These observations trace the water production rates (through its photodissociation product OH) and the coma expansion velocity. They are precious for statistical investigations of the evolution of the activity of the comets.

These observations are also made as a participation to multi-wavelength observing campaigns of dedicated comets and as a support to cometary space missions.

The observations are organized in a database which is progressively made publicly available: http://www.lesia.obspm.fr/planeto/cometes/basecom/ [1]

The most recent observations are listed in Table 1. Here are some recent highlights:

103P/Hartley 2 was observed in support to its fly-by by the *EPOXI* mission and to observations with *Herschel*. [2]

The outbursts of the sungrazing comet C/2012 S1 (ISON), preceding its demise as it approached the Sun at 0.012 AU on 28 November 2013, were observed. [3]

Comet C/2013 A1 (Siding Spring) was detected just before it passed at only 0.001 AU from Mars on 19 October 2014, due to enhanced background radiation as the comet was close to the Galactic plane. [4]

The Nançay radio telescope actively participated to the multi-wavelength observing campaigns of the bright comets C/2011 L4 (PANSTARRS), C/2012 F6 (Lemmon), C/2012 X1 (LINEAR), C/2013 R1 (Lovejoy) and C/2014 Q2 (Lovejoy) (Fig. 1), especially in coordination with radio observations with IRAM and ALMA.

It should be noted that the *Rosetta* target 67P/Churyumov-Gerasimenko, which was marginally detected at its 1982 passage due to a relatively close approach to Earth ($\Delta = 0.39$ AU) [1], is unfavourably placed at its present return for observations at Nançay.

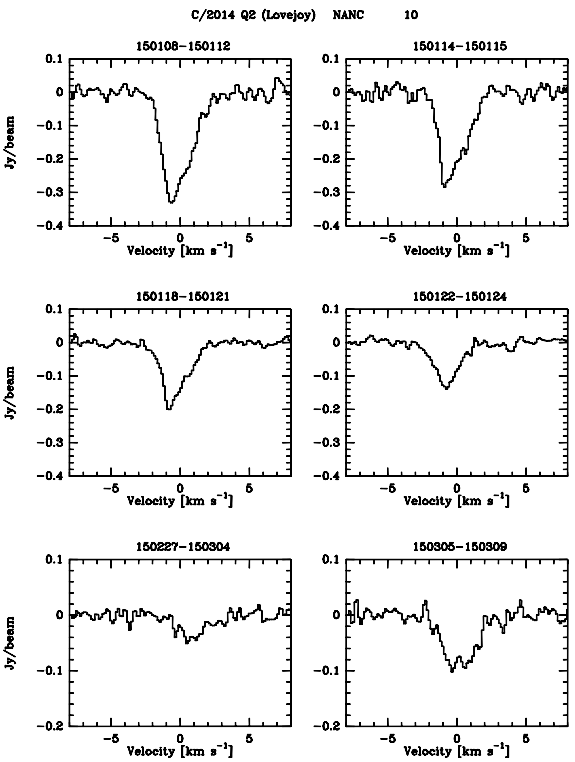

Figure 1: Sample spectra of C/2014 Q2 (Lovejoy) observed in January-March 2015.

References

[1] Crovisier, J., Colom, P., Gérard, E., Bockelée-Morvan, D., and Bourgois, G.: Observations at Nançay of the OH 18-cm lines in comets: The data base. Observations made

Table 1: Comets observed at Nançay since mid-2010.

comet	perihelion [yymmdd]	q [AU]	range of observations [yymmdd]	r_h range a) [AU]	N b)	c)	d)
C/2009 K5 (McNaught)	100430.03	1.422	100401–100414	1.44–1.48	7	L	D
C/2009 R1 (McNaught)	100702.16	0.401	100401–100831	0.41–1.92	60	L	D
10P/Tempel 2	100704.86	1.424	100422–100730	1.42–1.61	54	J	D
103P/Hartley 2	101028.50	1.058	100803–110131	1.06–1.63	113	J	D
C/2010 X1 (Elenin)	110910.74	0.482	110527–111023	0.48–2.09	54	L	D
45P/Honda-Mrkos-Pajdusakova	110928.78	0.530	110723–110916	0.59–1.34	21	J	D
C/2009 P1 (Garradd)	111224.03	1.550	110701–120330	1.57–2.75	117	L	D
96P/Machholz 1 (2012)	120714.78	0.124	120616–120811	0.14–0.88	26	H	M
C/2012 K5 (LINEAR)	121128.69	1.142	121220–131113	1.19–1.36	14	L	M
C/2011 F1 (LINEAR)	130108.04	1.118	121031–121221	1.83–2.01	23	L	D
C/2012 T5 (Bressi)	130224.17	0.323	130102–130214	0.43–1.29	29	L	–
C/2011 L4 (PANSTARRS)	130310.14	0.302	120901–130510	0.30–3.35	115	L	D
C/2012 F6 (Lemmon)	130324.52	0.731	130313–130428	0.76–1.00	18	L	D
C/2012 S1 (ISON)	131128.78	0.012	130708–131209	0.06–3.00	82	L	D
C/2013 R1 (Lovejoy)	131222.94	0.817	131101–140223	0.81–1.24	57	L	D
C/2012 X1 (LINEAR)	140221.64	1.599	131026–140508	1.62–2.22	54	L	D
C/2014 E2 (Jacques)	140702.50	0.665	140501–140919	0.67–1.77	64	L	D
C/2013 UQ4 (Catalina)	140706.00	1.081	140615–140630	1.09–1.13	5	H	–
C/2012 K1 (PANSTARRS)	140827.63	1.055	140403–140927	1.05–2.44	68	L	D
C/2013 V5 (Oukaimeden)	140928.17	0.627	140716–141024	0.63–1.55	40	L	D
C/2013 A1 (Siding Spring)	141025.39	1.399	141005–141220	1.43–1.61	22	L	D
C/2014 Q2 (Lovejoy)	150130.09	1.291	141221–150330	1.29–1.56	51	L	D

a) Lowest and highest heliocentric distance of the observations.
b) Number of observations in the data base.
c) L: long-period comet; H: Halley-family comet; J: Jupiter-family comet.
d) –: no detection; M: marginal detection; D: clear detection.

from 1982 to 1999. Astron. Astrophys., 393, 1053–1054, 2002.

[2] Crovisier, J., Colom, P., Biver, N., Bockelée-Morvan, D., and Boissier, J.: Observations of the OH 18-cm lines of Comet 103P/Hartley at Nançay in support to the EPOXI and Herschel missions. Icarus, 222, 679–683, 2013.

[3] Crovisier, J., Colom, P., Biver, N., and Bockelée-Morvan, D.: Comet C/2012 S1 (ISON). IAU Elect. Tel. No 3711, 2013.

[4] Crovisier, J., Colom, P., Biver, N., and Bockelée-Morvan, D.: Comet C/2013 A1 (Siding Spring). IAU Elect. Tel. No 4001, 2014.

EPSC Abstracts
Vol. 10, EPSC2015-824-1, 2015
European Planetary Science Congress 2015

Some properties of the distribution of long period comets.

M. Fouchard (1), H. Rickman (2,3), G. B. Valsecchi (4,5) and Ch. Froeschlé (6)
(1) LAL-IMCCE, Universit´e de Lille 1, 1 Impasse de l'Observatoire, F-59000 Lille, France (marc.fouchard@obspm.fr), (2) PAS Space Research Center, Bartycka 18A, PL-00-716, Warszawa, Poland (3) Dept. of Physics & Astronomy, Uppsala Univ., Box 516, SE-75120 Uppsala, Sweden (Hans.Rickman@physics.uu.se), (4) IAPS, INAF, via Fosso del Cavaliere 100, I-00133 Roma, Italy (giovanni@iaps.inaf.it) (5) IFAC-CNR, Via Madonna del Piano 10, I-50019 Sesto Fiorentino (FI), Italy, (6) Observatoire de la Côte d'Azur, UMR Lagrange 7293, Bv. de l'Observatoire, B.P. 4229, F-06304 Nice cedex 4, France (froesch@oca.eu)

Abstract

The scope of the present study is to compare the flux of observable long period comets obtained numerically to the observed flux of long period comets. Such comparison should give us some hint about the incompleteness of the observed flux with respect to the perihelion distances, the validity of the injection scenario toward the observability, and to make some hypothesis on the recent past history of the observed long period comets. In addition, if our numerical data are statistically reliable it should be possible to investigate some fading laws for these comets.

1. Introduction

We have modelled the dynamics of 10^7 Oort cloud comets over the age of the solar system using the model described in [1, 2, 3]. The final flux of observable comets with original semi-major axis greater than 10 000 AU has been computed. This flux has been weighted considering a present flux of 4 comets per year for perihelion distance smaller than 5 AU with a total absolute magnitude HT < 11 over 25 years [5] (from 1990 until present time).

For comparison, the JPL Horizon system [4] has been used to compute the original barycentric orbital elements, i.e. at 150 AU from the Sun before perihelion, of all long period comets discovered after 1990, January 1st, with perihelion distance smaller than 5 AU and original semi-major axis greater than 10 000 AU.

2. Preliminary figures

Fig. 1 shows the shape of the Oort peak, i.e. the distribution of orbital energy of observable comets, and Fig. 2 the distribution of perihelion distances. For both figures, the bin are coloured according to the proportion of comets in the following four different dynamical classes : the *jumpers*, for which the preceding perihelion passage was at more than 15 AU from the Sun (in red on the figures), otherwise the comet is a *creeper*. In addition if at the preceding perihelion passage a planetary perturbation has significantly increased the orbital energy of the comet then the comet is classified as a *Kaib and Quinn jumper* or *Kaib and Quinn creeper* comet.

On each plot, the distribution obtained from the JPL Horizon system [4] is also plotted.

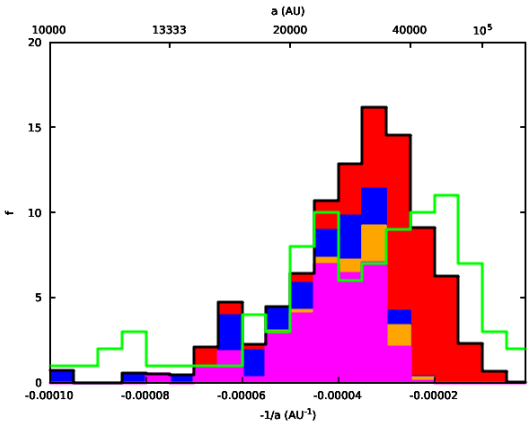

Figure 1: Distribution of orbital energy of observable long period comets. The coloured are of each bin is proportion to the proportion of comets in the corresponding classes : red for jumpers, orange for Kaib and Quinn jumpers, magenta for Kaib and Quinn creepers, and blue for creepers (see text the main text for the definition of the classes). The green line corresponds to the distribution obtained from the JPL-Horizon system [4].

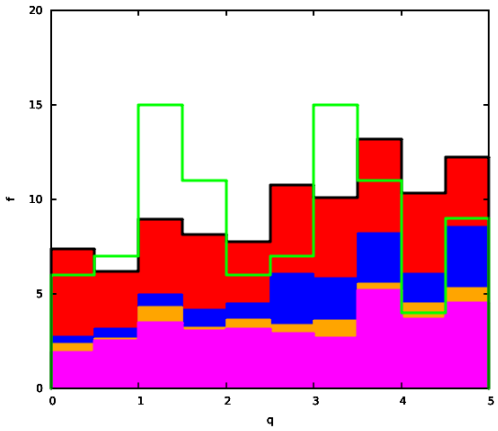

Figure 2: Distribution of perihelion distance for observable long period comets. The color are the same as for Fig. 1.

3 Perspectives

We aimed to used such kind of comparison to deduce some information about the completeness of detection of long period comets with respect to perihelion distance and to make some hypothesis on the recent past history of individual known long period comets. Considering also the observable long period comets with semi-major axis smaller than 10 000 AU, it should be possible to estimate some fading law for these comets.

References

[1] H. Rickman, M. Fouchard, Ch. Froeschlé, G. B. Valsecchi, Injection of Oort Cloud comets: the fundamental role of stellar perturbations, Celest. Mech. and Dynam. Astron. 102 (2008) 111–132.

[2] M. Fouchard, Ch. Froeschlé, S. Breiter, R. Ratajczak, H. Valsecchi, G.B. Rickman, Methods to Study the Dynamics of the Oort Cloud Comets II: Modelling the Galac- tic Tide, in: D. Benest, C. Froeschlé, E. Lega (Eds.), Top- ics in Gravitational dynamics, vol. 729 of Lecture Notes in Physics, Berlin Springer Verlag, 271–293, 2007.

[3] M. Fouchard, H. Rickman, C. Froeschlé, G. B. Valsecchi, Planetary perturbations for Oort Cloud comets. I. Dis- tributions and dynamics, Icarus 222 (2013) 20-31.

[4] Giorgini, J.D., Yeomans, D.K., Chamberlin, A.B., Chodas, P.W., Jacobson, R.A., Keesey, M.S., Lieske, J.H., Ostro, S.J., Standish, E.M., Wimberly, R.N., "JPL's On-Line Solar System Data Service", Bulletin of the American Astronomical Society 28(3), 1158, 1996.

[5] P. J. Francis, The Demographics of Long-Period Comets, APJ 635 (2005) 134-1361.